INL/CON-05-00259
PREPRINT

Laser Measurement Of SAM Bulk and Surface Wave Amplitudes For Material Microstructure Analysis

22nd Annual Review of Progress in Quantitative Nondestructive Evaluation

C. Miyasaka
K. L. Telschow
D. L.Cottle

July 2005

LASER MEASUREMENT OF SAM BULK AND SURFACE WAVE AMPLITUDES FOR MATERIAL MICROSTRUCTURE ANALYSIS

C. Miyasaka, K. L. Telschow[1], and D. L. Cottle

Physics Department, Idaho National Laboratory, Idaho Falls, ID 83415, USA

ABSTRACT. We present a hybrid acoustic imaging technique to directly visualize acoustic waves propagating within a thin silicon plate. A high frequency acoustic point focus lens was used to form a small point source within the plate. A laser interferometric system was used to visualize the acoustic wave propagation. Distinct amplitude patterns at each focal plane were experimentally visualized. The measured amplitude patterns exhibited the cubic symmetry of the material and the effects of focusing of the source outside and inside the material.

Keywords: Laser Based Ultrasonics, Acoustic Lens, Angular Spectrum
PACS: 07

INTRODUCTION

The mechanical scanning acoustic reflection microscope (hereinafter called simply "SAM") operating with frequencies substantially ranging from 0.1 to 2.0 GHz has proven to be a useful apparatus for characterizing of anisotropic materials on the scale of individual grains [1,2,3]. Note that the SAM is basically designed to visualize the surface and/or the subsurface of microstructure features of the material, but not directly the acoustic waves propagating within the material. However, observing a wave front traveling within the material would be significant for understanding physical phenomena, such as scattering from microstructure features [4,5,6,7]. In addition, visualization of the acoustic wave front can help in measurement of elastic properties and improve quality evaluation of an acoustic lens.

In this article, we present a hybrid technique (*i.e.*, integration of laser based acoustic microscopy and scanning acoustic microscopy) to directly visualize wave front amplitudes of acoustic bulk and surface waves emanating from a focused source outside and inside a material sheet. An ultrahigh frequency (~200 MHz) acoustic lens tightly focused compression waves onto the back surface of a thin silicon plate, crystalline plane (100) oriented with its normal to the plate surface, via a coupling medium (*i.e.*, water). A laser beam focused onto the front surface of the specimen via an optical objective lens included in the laser interferometric system detected the amplitudes of the bulk and surface acoustic waves at the front surface of the plate. Distinct symmetric amplitude

[1] Correspondence: E-mail: kenneth.telschow@inl.gov; Tel: (208) 526-1264; Fax: (208) 526-0690

patterns that altered in predictable ways, as the acoustic focal point moved toward the front surface of the plate, were observed. Predictions of the acoustic wave fields generated by the acoustic lens within the plate are being investigated with an Angular Spectrum of Plane Waves method for an anisotropic crystalline solid [8,9,10].

DESCRIPTION OF THE OPTOACOUSTIC SYSTEM

Figure 1 illustrates a schematic diagram of the experimental measurement. The optoacoustic system comprises a computer for controlling all operations and data acquisition, a laser interferometric system based on the photorefractive effect, a detachable revolving nosepiece including optical objective lenses, and an inverted SAM including a receiver and/or transmitter, and a specimen holder allowing x-y-z motions.

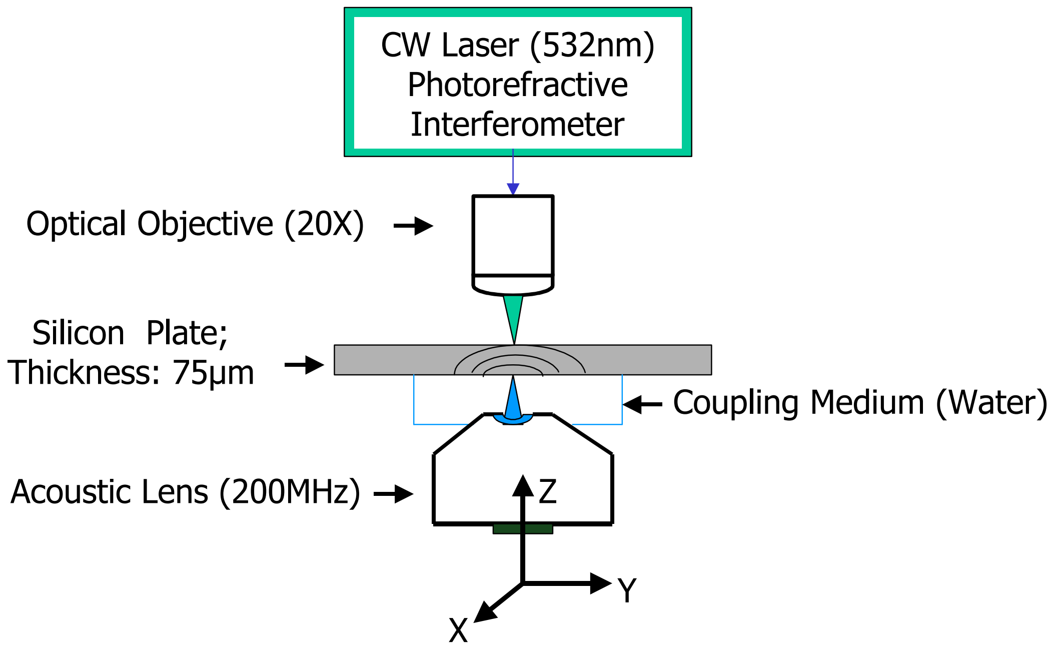

Figure 1. A schematic diagram of an optoacoustic system.

An acoustic lens was used to form a point focus within the specimen. The point focus acoustic lens comprises a piezoelectric transducer (*i.e.*, zinc oxide) and a buffer rod made of a single crystal of sapphire. The piezoelectric transducer located on the top of the buffer rod was driven in the continuous wave mode at a single frequency. The excitation voltage at the transducer was approximately 5 volt peak-to-peak. The electrical signal was converted into an acoustic signal (*i.e.*, ultrasonic plane wave) by the transducer. The shape of the transducer was circular with a diameter of 1mm and a thickness of about 10 µm respectively. The maximum output from the transducer was measured at 185 MHz. The ultrasonic plane wave traveled through the buffer rod to a spherical recess (hereinafter called simply the "lens") located at the bottom of the buffer rod. The lens contained a silicon-oxide layer to form an acoustic impedance matching layer (*i.e.*, acoustic anti-reflection coating) for coupling into water. The diameter of the lens aperture was 843 µm, the aperture angle 120º, and the working distance was 310 µm.

A thin (100) silicon plate (thickness 75 µm) was used as a specimen. The back surface of the specimen was above the lens with its normal along the lens Z-axis. The front and back surfaces of the specimen had been mechanically polished to provide a well characterized boundary. The ultrasonic beam was focused onto a predetermined interior or exterior plane of the specimen by controlling the standoff distance between the lens and the back surface. A special filling apparatus was designed to keep the water coupling in place over periods of a week or more with out refilling. The water temperature was substantially kept at 23ºC.

The laser interferometer utilized a CW 532 nm Nd:YAG laser and a photorefractive interferometer based on Bismuth Silicon Oxide [4]. Data acquisition was synchronized to the source excitation so that complete determination was made of the ultrasonic normal displacement amplitude and phase spatially along the sample front surface plane. With a 20X optical objective, the field of view was about 300 µm, and the spatial resolution was on the order of 1-2 µm.

EXPERIMENTAL MEASUREMENT RESULTS

Figure 2 shows the focusing geometry for the measurements, defining the standoff distance Z_F. This distance was varied to change the acoustic lens focal point from outside to inside the material plate. The zero point for Z_F is a location about 600µm below the plate front surface, as shown. When $Z_F = +200$ µm, the focal point is calculated to be at the plate back surface. At each standoff distance, the ultrasonic displacement was recorded at the plate front surface by scanning the sample under the optical objective. Although the system employed can image the data without scanning, the low signal to noise level observed precluded imaging for the excitation levels employed.

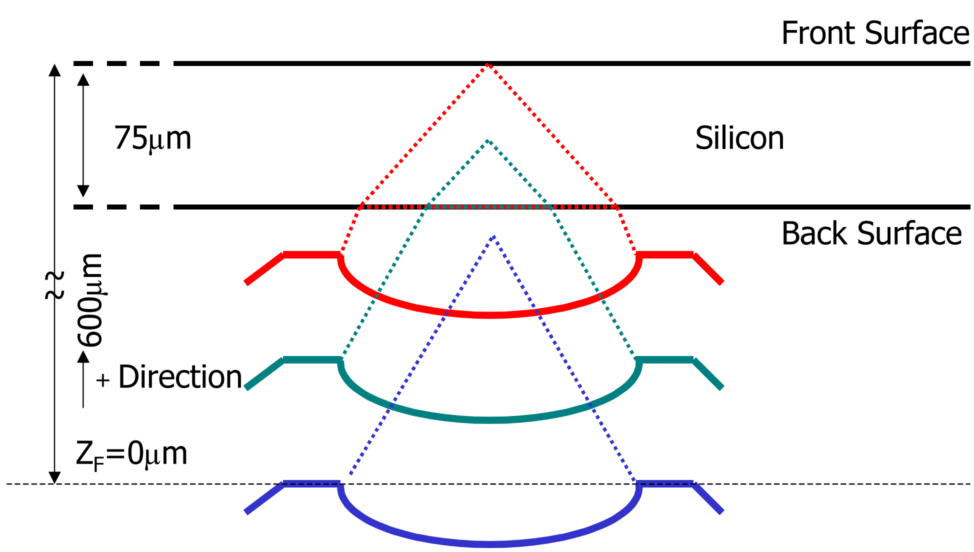

Figure 2. Focusing geometry showing the focal distance variable Z_F that is varied from –891µm to +300µm to produce focal points outside and inside the material plate. The origin $Z_F = 0$ is 600µm from the front surface of the silicon plate.

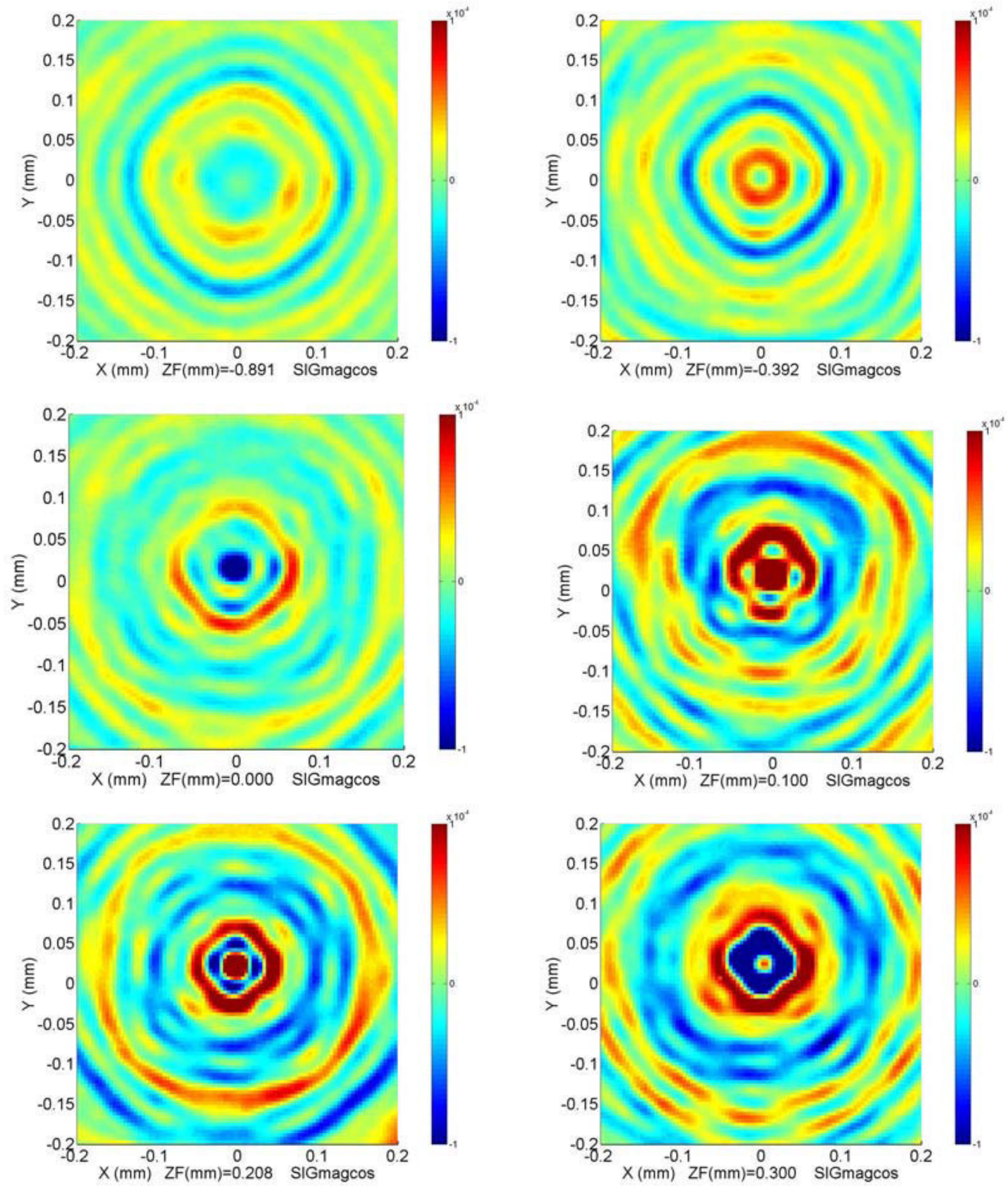

Figure 3. Images of the ultrasonic motion (magnitude x cosine(phase)) at the surface as the standoff distance Z_F is changed as indicated.

Figure 3 shows images of amplitudes of acoustic waves propagating on the front surface of the specimen in accordance with the change of the focal plane due to the position of the acoustic lens (Z_F). The images show the product of the displacement magnitude times the cosine of the phase to illustrate the amplitude and phase changes observed. Figure 3(e) is the image when the acoustic lens is substantially focused onto the back surface of the specimen. The focal beam spot (the circle at the center) having the maximum intensity is clearly observed. Figure 3(f) is the image when the acoustic lens is mechanically moved 98 μm toward the front surface from the back surface plane, which would place the focal point above the front surface. Since the aperture angle of the

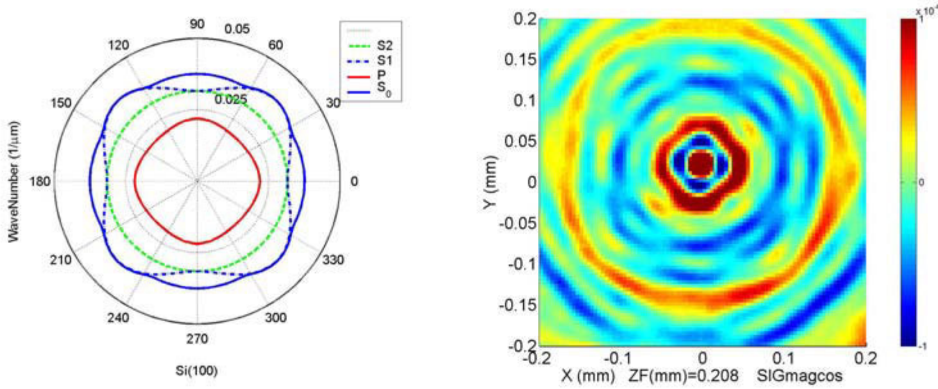

Figure 4. (left) Calculated wavenumbers for the bulk longitudinal (P), bulk shear (S1, S2) and symmetric plate (S_0) modes of the 75μm Silicon (100) plate at 185 MHz, and (right) the acoustic amplitude image for the case when the focal point is near the top surface of the plate.

lens is large, longitudinal, shear and surface acoustic waves are all generated when defocusing the lens toward the specimen. Also, since the excitation is continuous, plate wave modes are present due to multiple reflections from the surfaces. Figure 3(f) shows all wave amplitudes simultaneously; therefore, only through mathematical modeling can discrimination be accomplished between the various types of waves shown in the image.

Figure 4 shows the phase velocities and wave slowness diagrams for Si(100) and illustrates the variety of wave propagations possible. Also shown is the slowness diagram for S_0 mode plate waves as a function of propagation direction along the plate surface. At the high frequency employed, the $S_{0,}$ A_0 and Rayleigh modes all coincide. The images of the acoustic wavefronts have essentially the same symmetry properties as the wavenumber as a function of propagation direction, since the material is cubic. Comparison of the acoustic displacement amplitude with the wavenumber prediction for Si(100) shows this similarity in Fig. 4.

THEORETICAL APPROACH

Work is in progress to predict the acoustic wave amplitude at the surface of the silicon plate taking into account all the modes excited through the "Angular-Spectrum of Plane Waves" approach [10]. If the wave amplitude or stress distribution is known on any plane, then the corresponding wave amplitude or stress can be calculated on any other parallel plane through a summation of plane waves propagating form one plane to the other. Each plane wave component must be a solution to the appropriate wave equation for the medium through which it travels. Since the angular frequency and the parameters of the acoustic lens are known, the acoustic field focused on the back surface plane can be calculated. The summation must occur over all in-plane components of wavenumber and include propagating as well as non-propagating wavevectors. The main complication to this approach is that the Christoffel equation must be solved for the z-component of the wavevector that satisfies for the frequency used and all the in-plane wavevector components. In this way the acoustic displacement amplitude on any plane in the water and inside or at the surface of the silicon plate can be calculated. The results of this calculation shall be presented in a future publication.

POTENTIAL APPLICATIONS

The hybrid technique (*i.e.*, integration of laser based acoustic microscopy and scanning acoustic microscopy) presented offers potential for extending the capabilities of acoustic microscopy. In particular, the ability to directly visualize the acoustic displacement output from the transducer will allow the data to be back-propagated to the transducer using the Angular Spectrum of Plane Waves technique. In this way, a direct measure of the actual "V(z) curve" is obtained for the geometry and sample used. V(z) curves can then be directly predicted for anisotropic as well as inhomogeneous specimens and for characterizing the transducer and buffer rod itself.

CONCLUSIONS

We presented a hybrid acoustic imaging technique to directly visualize amplitude of acoustic waves propagating within a thin silicon (100) plate as a complimented approach to the conventional SAM. The technique comprises a laser based acoustic microscopy and a mechanical scanning acoustic reflection microscopy. A high frequency acoustic point focus lens (200 MHz) was used to form a small point source within the plate. Distinct symmetric amplitude patterns were observed as the acoustic focal point moved toward the front surface of the plate. We are planning to use a newly designed acoustic lens for generating large amplitude of ultrasonic waves with higher frequency to form their clearer visualization without mechanical scanning.

We have also developed a mathematical model (*i.e.*, a method of angular spectrum for a plane wave) to calculate an elastic wave field for prediction of acoustic behavior of isotropic and/or anisotropic materials. The computer simulation results based on the model shall be compared to the experimental results in the near future.

ACKNOWLEDGEMENTS

This work was supported by U.S. Department of Energy, Office Basic Energy Sciences, Materials and Engineering Physics under DOE Idaho Operations Office Contract DE-AC07-99ID13727. The authors would like to thank Mr. Rob Schley at Idaho National Laboratory for designing and fabricating the water couplant filling apparatus for these measurements.

REFERENCES

1 C. F. Quate, “Acoustic Microscopy,” *Physics Today*, Vol. 38, pp. 34-42, (August 1985).

2 N. Chubachi, “Ultrasonic Micro-Spectroscopy via Rayleigh Waves,” in *Rayleigh-Wave Theory and Application*, edited by E. A. Ash and E. G. S. Paige, Proceedings of an International Symposium Organized by the Rank Prize Funds at the Royal Institution, London 15-17 July, 1985, pp. 291-297.

3 J. Kushibiki, N. Chubachi, “Material Characterization by Line-Focus-Beam Acoustic Microscope,” *IEEE Trans.* **SU-32**(2), pp. 189-212, (March 1985).

4 K. L. Telschow, “Full-Field Imaging of Gigahertz Film Bulk Acoustic Resonator Motion,” *IEEE Trans.* **50**(10), pp. 1279-1285, (October 2003).

5 K. L. Telschow, V. A. Dearson, D. L. Cottle, and J. D. Larson III, “Full-Field Imaging of Acoustic Motion at Nanosecond Time and Micron Length Scale,” in 2002 *IEEE Ultrasonics. Symposium,* pp. 601-604, (2002).

6 K. L. Telschow, V. A. Dearson, D. L. Cottle, and J. D. Larson III, “UHF Acoustic Microscopic Imaging of Resonator Motion,” in 2000 *IEEE Ultrasonics. Symposium,* pp. 631-634, (2000).

7 K. L. Telschow, V. A. Dearson, R. S. Schley, and S. M. Watson, “Direct Imaging of Lam Waves in Plates using Photorefractive Dynamic Holography,” *J. Acoust. Soc. Am.*, **106**(5)*,* pp. 2578-2587, (1999).

8 M. F. Hamilton, Yuri A. Il’inskii, and E. A. Zabolotskaya, “Nonlinear Surface Acoustic Waves in Crystals,” *J. Aoust. Soc. Am.* 105(2), pp. 639-651, (February 1999).

9 D. J. Vezzetti, “Propagation of Bounded Ultrasonic Beams in Anisotropic Media,” *J. Aoust. Soc. Am.* **78**(3), pp 1103-1108, (September 1985).

10 A. Atalar, “An Angular-Spectrum Approach to Contrast in Reflection Acoustic Microscopy,” *J. Appl. Phys*., **49**(10), pp. 5130-5139, (October 1978).